JJEE
Volume 3, Number 2, 2017
Pages 86-101
Jordan Journal of Electrical Engineering
ISSN (Print): 2409-9600, ISSN (Online): 2409-9619

Anti-Sway System for Container Cranes with Coordinated Motion Control and Reduced Dynamic Loads

Kamal Khandakji[1], Victor Busher[2], Lubov Melnikova[2]

[1]Department of Electrical Power Engineering and Mechatronics, Tafila Technical University, Tafila, Jordan
[2]Department of Electromechanical Systems with Computer Control, Odessa National Polytechnic University, Odessa, Ukraine

Received: February 16, 2017 *Accepted: April 27, 2017*

Abstract— A novel anti-sway control system for cranes is proposed. The proposed method is based on the formation of a predetermined sway angle as a piecewise-continuous function, the second derivative of which does not experience discontinuity. Its third derivative is a rectangular pulse of certain variable-sign amplitude, which results in eliminating the mechanical stress in the crane construction and kinematic gears. A comprehensive mathematical model and an experimental prototype of the crane are developed. Simulation and experimental results prove that the proposed anti-sway method enables damping of the oscillations of the suspended load during its horizontal motion (in two orthogonal coordinates) and hoisting/lowering. The control method is invariant to the mechanism/load mass ratio, lift height and hoisting speed.

Keywords— Anti-sway system, Container crane, Motion control, Oscillations damping.

I. INTRODUCTION

A rapid and reliable operation of harbor and ship-to-shore container cranes has a significant impact on a port terminal efficiency. The improvement of a crane performance requires studying and deep analysis of the crane operation in both steady-state and dynamic modes of operation. Thus, several mathematical models of different levels of complexity have been created to simulate the operation of different types of cranes [1]-[11].

The major part of a loading/unloading cycle of such cranes is travelling; i.e. moving the load along the boom from the ship to the shore and vice versa. With lift heights 20-50 m, trolley travelling mechanisms are characterized by relatively long transients due to the sway of the suspended load; damping such oscillations may take 20-30s. Thus, including anti-sway control is mandatory for a reliable and efficient crane operation.

Various anti-sway control systems have been developed to mitigate load oscillations during the operation of cranes. In the last decade a dynamical nonlinear model of the crane was implemented to suppress the cargo swaying [12], [13]. A rate-based control strategy was developed in [14] to directly compute required crane joint rates to isolate the payload from the ship motion using only inertial measurement unit information. Pontryagin's Principle with constant force and step-change switching technique was used implemented in [15].

The implementation of input-shaping in the anti-swinging control was achieved in [16] using the on-line two-dimensional inclinometer measurements and an on-line calculation of input impulse trains. The developed input-shaping control was divided into two phases: straight line motion and external perturbances cancellation. An adaptive fuzzy sliding-mode control (AFSMC) was presented in [17] for the robust antisway trajectory tracking of overhead cranes subject to both system uncertainty and actuator nonlinearity. In [18], a nonlinear tracking control law was implemented to eliminate the nonlinear characteristics of the system and achieve the satisfactory position control and swing suppression, in the presence of the initial swing angle and the variation of payload weight. An integrated computer simulator tool of

Corresponding author's e-mail: drkhandakji@yahoo.com

rotary crane with ship behavior was considered as ship sway and load sway in [19]. The integrated simulator was realized by corporating an external force interface routine of a component with fluid analysis software. In [20], an anti-swing controller using a dual stage control system is proposed. System parameters are characterized by a system identification process with respect to the 1/20 scale D4 crane model and the LQR controller. Anti-swing was designed based on decoupled of *X*- and *Y*-axis and linearized crane model.

Recently, a sliding-mode control for container cranes is discussed in [21]-[24]. A sliding surface is designed in such a way that the sway motion of the payload is incorporated into the trolley dynamics; the control law is of a varying gain. An adaptive version of the sliding mode control of a crane system is developed in [23], considering the case of no prior knowledge of the payload mass and damped elements. Using two inputs, namely, trolley driving force and cargo lifting force, the proposed adaptive robust controller simultaneously executes four duties including tracking the trolley, hoisting the cargo, keeping the cargo swing small during the transient state, and completely eliminating the payload angle at a steady destination.

Model predictive control (MPC) controller provides fast transfer of cargo with sway reduction in [25]. The solution for criterion function of MPC controller was reached through multicriteria optimization. In [26], the finite-time regulation controller for the underactuated crane systems in 2-dimensional (2D) space with both constant cable length and varying cable length is considered. The designed controller can simultaneously suppress the payload swing and regulate the trolley to the desired destination within a finite time for the 2D bridge crane system in the case of constant cable length.

In [27], it is shown that the load oscillatory behavior depends on the length of the rope; thus, a gain-scheduling control law is proposed to reduce such an effect. To take into account the technological limits in the controller implementation, a fixed-order controller is tuned by enforcing robustness and performance constraints.

One possible method to solve the anti-sway problem is to implement Pontryagin's Principle [15], [28], which takes into account the constraints on the control inputs supplied to the control object, and gives the most effective results in the synthesis of the optimum response of a system. However, the resulting solutions with multiple switching control between the maximum and minimum values require an accurate measurement of the mass ratio of the load and its mechanism, and the instantaneous height of the suspended load and its persistence during the transition process. In practice, such restrictions impose additional requirements on the used equipment, and hinder the freedom of action of the operator. Therefore, successful damping of the load oscillations requires the use of such a control methodology that allows the simultaneous operation of multiple mechanisms (horizontal travelling and lifting). On the other hand, the control methodology should be least sensitive to the errors of the measured parameters of the load and to any possible random disturbances.

II. MOTION MODEL OF TROLLEY AND LOAD

The mathematical model of the travelling mechanism of the trolley or the horizontal motion of the crane can be represented by a two-mass mechanical system with an inextensible imponderable rope length of *L*. Taking into account the simplified assumption made for most industrial cranes $(\sin\alpha \approx \alpha, \cos\alpha \approx 1)$, the dynamics in this model can be described using the following system of differential equations:

$$
\begin{aligned}
a_1 &= \frac{F(t)}{m_1} - g\frac{m_2}{m_1}\alpha, \\
\frac{dv_1}{dt} &= a_1, \\
\frac{ds_1}{dt} &= v_1, \\
a_2 &= g\alpha, \\
\frac{dv_2}{dt} &= a_2, \\
\frac{ds_2}{dt} &= v_2, \\
\alpha &= \frac{s_1 - s_2}{L},
\end{aligned}
\tag{1}
$$

where $a_1, v_1, s_1, a_2, v_2, s_2$ are acceleration, linear speed and displacement of the suspension point 1 and load 2, respectively; α is the load sway angle, i.e. the angle of deviation of the rope from the vertical; $F(t)$ is the force produced by the electric drive; which is the control action on the suspension point (Fig. 1).

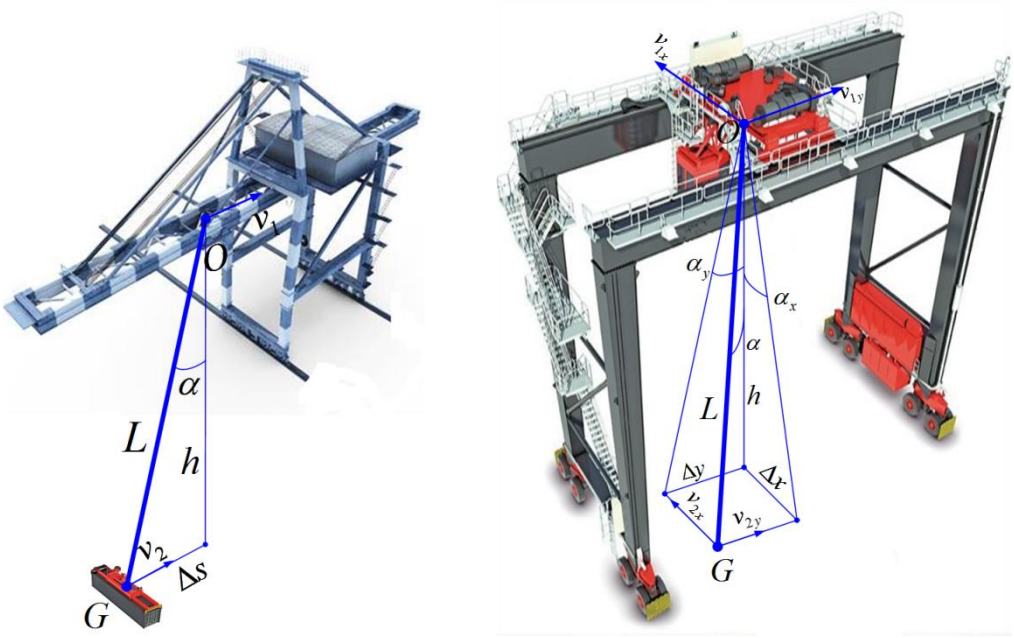

a) b)

Fig. 1. Main parameters that characterize the process of swinging in cranes: a) with longitudinal movement of the cargo along the console (ship to shore container crane), b) with combined movement operations (rear container crane)

III. ANTI-SWAY DYNAMICS AND CONTROL

The control objective is to create such a coordinate control law that ensures the absence of the load swinging by the end of a transient of the travelling process. One of the invariant methods to the ratio of the masses of the moving part of the crane and the load controls the speed of the load suspension point with a certain function. In this method with a predefined function of α from (1), the load speed $v_2(t)$ can be defined as the integral of $\alpha(t)$:

$$
v_2(t) = g\int_0^t \alpha(t)\,dt, \tag{2}
$$

Differentiating the equation $\alpha L = s_1 - s_2$, the function of the speed of the suspension point is obtained:

$$v_1(t) = v_2(t) + \frac{d(\alpha(t)L(t))}{dt} = g\int_0^t \alpha(t)dt + \alpha(t)\frac{dL(t)}{dt} + L(t)\frac{d\alpha(t)}{dt}. \quad (3)$$

In (3), a control method in which the angle α is defined by a continuous smooth twice the differentiable function is chosen; the function should have zero initial and final conditions, including the first derivative. One of the set of such functions is, for example, the harmonic function:

$$\alpha = \alpha_m\left(1 - \cos\left(\frac{t}{T_G}\right)\right), \quad (4)$$

where α_m is half of the maximum angle of the vertical deviation of the rope; T_G is time constant, inverse of the angular frequency of the load oscillations.

According to (4), with small values of the deviation angle $(\sin\alpha \approx \alpha, \cos\alpha \approx 1)$ the speed of the load from the initial value V_0 to the final V_E changes according to the following function:

$$v_2(t) = V_0 + \alpha_m g t - \alpha_m g T_G \sin\left(\frac{t}{T_G}\right), \quad (5)$$

where $\alpha_m g = a$ is the average acceleration of the load and the trolley during one period of oscillations.

The speed of the suspension point in general must satisfy the condition:

$$v_1(t) = v_2(t) + \frac{d(\alpha L)}{dt}. \quad (6)$$

Thus, if acceleration can be calculated according to the following formula:

$$a = \frac{V_E - V_0}{2\pi T_G}, \quad (7)$$

Then, after a time $t = 2\pi T_G$, we obtain $\alpha = 0$, $\frac{d\alpha}{dt} = 0$, $v_1 = v_2 = V_E$.

If the value of $2a$ exceeds the acceleration limit, it should be noted that at $t = \pi T_G$ the angle α reaches its maximum value $\alpha = 2\alpha_m$; and the acceleration of the load reaches its maximum and equals $2\alpha_m g$. If at this time the acceleration of the trolley is changed to the value of the load acceleration, then the deviation angle α will remain constant.

Thus, the control law of the travelling mechanism consists of three stages: 1) acceleration from initial state $\alpha = 0$ to the predetermined set point speed, which is achieved with zero deviation of the load from the vertical; 2) steady-state operation with the set point speed with $\alpha = 0$; 3) braking till standstill, which is reached with zero load deviation from the vertical.

The duration of the transient is short if the duration of the first and third intervals are minimized. The average acceleration of the mechanism and load during these intervals is twice less than it in the second stage.

Based on the maximum permissible force $F_{\max}$, which is developed by the travelling drive, T_G should satisfy the following condition:

$$T_G \geq \sqrt{\frac{Lm_1}{2g\left(m_1+m_2\right)}}, \tag{8}$$

So, the duration of the second interval

$$t_2 = \frac{V_E - V_0}{2a} - \pi T_G, \tag{9}$$

The linear component of acceleration during the first and third intervals is $a = \frac{F_{\max}}{2\left(m_1+m_2\right)}$.

With fixed length of the ropes during the transient process, (5) and (6) show the speed of the suspension point for each of the three time intervals:

$$v_1(t) = \begin{cases} V_0 + at - \left(aT_G - \frac{aL}{gT_G}\right)\sin\left(\frac{t}{T_G}\right) \forall\ 0 \leq t \leq \pi T_G, \\ V_0 - a\pi T_G + 2at \ \forall\ \pi T_G < t \leq \pi T_G + t_2, \\ V_0 + a\left(t+t_2\right) - \left(aT_G - \frac{aL}{gT_G}\right)\sin\left(\frac{t-t_2}{T_G}\right) \forall\ \pi T_G + t_2 < t \leq 2\pi T_G + t_2. \end{cases} \tag{10}$$

The force developed by the traveling mechanism can be derived from (1):

$$\begin{aligned} F(t) &= m_1\frac{dv_1}{dt} + m_2\frac{dv_2}{dt} = \\ &= m_1\left(g\alpha + \alpha\frac{d^2L}{dt^2} + 2\frac{d\alpha}{dt}\frac{dL}{dt} + \frac{d^2\alpha}{dt^2}L\right) + g\alpha m_2, \end{aligned} \tag{11}$$

Respectively, for each of the three time intervals we obtain:

$$F(t) = a\begin{cases} m_1\left(\frac{L}{gT_G^{\ 2}}\cos\left(\frac{t}{T_G}\right) + \frac{v_L}{gT_G}\sin\left(\frac{t}{T_G}\right)\right) + \\ +m_2\left(1-\cos\left(\frac{t}{T_G}\right)\right) \forall\ 0 \leq t \leq \pi T_G, \\ 2\left(m_1+m_2\right) \forall\ \pi T_G < t \leq \pi T_G + t_2, \\ m_1\left(\frac{L}{gT_G^{\ 2}}\cos\left(\frac{t-t_2}{T_G}\right) + \frac{v_L}{gT_G}\sin\left(\frac{t-t_2}{T_G}\right)\right) + \\ +m_2\left(1-\cos\left(\frac{t-t_2}{T_G}\right)\right) \forall\ \pi T_G + t_2 < t \leq 2\pi T_G + t_2. \end{cases} \tag{12}$$

where $v_L = \frac{dL}{dt}$ is the speed of change of the ropes length, i.e. the hoisting/lowering speed. Taking $v_L = 0$, we obtain several characteristic values on the basis of which the required parameters of the transient process can be defined:

$$F(t)=\begin{cases} am_1\dfrac{L}{gT_G^{\,2}} \;\forall\; t=0,\; t=2\pi T_G+t_2, \\ 2a\left(m_1+m_2\right) \;\forall\; \pi T_G<t\le \pi T_G+t_2, \\ -am_1\dfrac{L}{gT_G^{\,2}}+2am_2 \;\forall\; t=\pi T_G,\; t=\pi T_G+t_2. \end{cases} \tag{13}$$

According to the maximum permissible force in the second interval $F_{\max}=2a\left(m_1+m_2\right)$, we get $a=\dfrac{F_{\max}}{2\left(m_1+m_2\right)}$ and the minimum duration of the first and third intervals $T_{G\min}=\sqrt{\dfrac{Lm_1}{2g\left(m_1+m_2\right)}}$.

Thus, the control law of the speed of the suspension point is obtained. Such a control law gives the opportunity of combining the hoisting and traveling operations; and it does not require an accurate measurement of the load mass. T_G can be chosen according to some limitations. The deviation of the mass from the calculated value leads to the change of the force during the transient.

Theoretically, though the load oscillations do not exist by the end of the mechanism acceleration, the real speeds of the load and its suspension point are coincided with the calculated values. Fig. 2 illustrates an implementation of the obtained speed control law (10) in a lowering transient process at 1m/s with an initial length of the ropes 35m and horizontal motion in x, y coordinates simultaneously.

The time intervals $\pi T_{G_x}, t_{2_x}, \pi T_{G_y}, t_{2_y}$, which can vary due to different parameters of electric drives and mechanisms, are shown. Obviously, residual vibrations ($\Delta x, \Delta y$) are absent.

It is obvious that the predicted behavior of the cargo allows for the automation of the crane operation by implementing positioning at predetermined points.

It should be noted that the use of the cosine function (4) for the angle of deviation of the load results in a necessity of step change in the motor torque/force by a value of $\pm F_{\max}$ several times during the transition (13). Such a control law inevitably leads to a mechanical surge that may cause damage and reduce the life of the mechanical transmission and motor.

IV. ANTI-SWAY CONTROL IMPROVEMENT AND SIMULATION

The function of deviation of the load angle should be modified to eliminate the impermissible mechanical stresses on the motor shaft using a physically realizable torque law which can be implemented in modern variable frequency electric drive (VFD) or direct torque control (DTC) systems. It ensures the condition of damping the oscillations of the suspended load when any combined vertical and horizontal motion of the load is possible in container cranes.

To prevent such negative phenomena as well as to produce a physically realizable torque law compatible with VFD or DTC, it is necessary to form such a function $\alpha(t)$ that meets the condition of continuity and twice differentiability. For this condition, ideal rectangular pulses of variable-sign torque are not required to be produced by the motor.

In accordance with (2), (3) and (12), a control method based on the formation of a predetermined deviation angle, as a piecewise continuous function, the second derivative of which is continuous, can be proposed.

Then, forming the third derivative of $\alpha(t)$ in a rectangular form of fixed amplitude and width and a variable sign on the initial sections of acceleration and deceleration, the change of the second derivative can be provided in a form of a trapezoid. This in turn determines the shape

of the first derivative of a curve consisting of parabolas at the initial and final sections and a middle linear section.

Thus, the shape of the curve $\alpha(t)$ contains cubic parabolas in the initial and final sections in conjunction with linear sections when increasing and maintaining the deflection angle of the load. Fig. 3 shows the initial part of this process, which corresponds to the interval πT_G of Fig. 2. Also, Fig. 4 shows a comparison of sway angles using the proposed anti-sway method in this paper (curve 1) and the neural anti-sway method with PSO (curve 2) proposed in [29]. It can be seen that both methods keep the load sway angle constant by the end of the transient. But during the transient, the proposed system has minimum sway angle fluctuations at the beginning of the traveling process; the sway angle is kept constant during traveling before it vanishes by the end of the process as shown in Fig. 5.

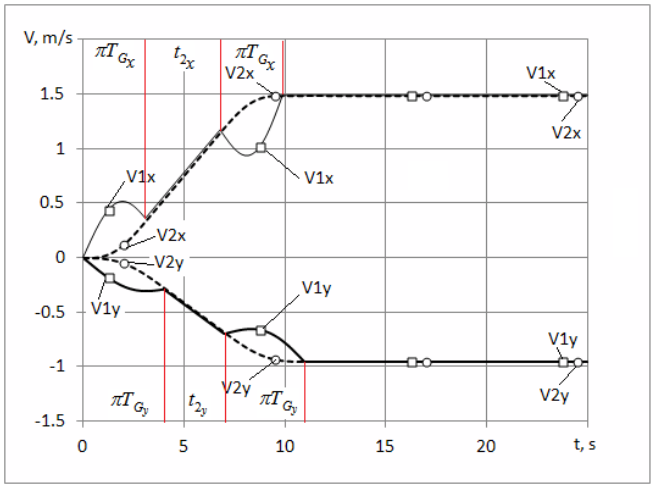

a)

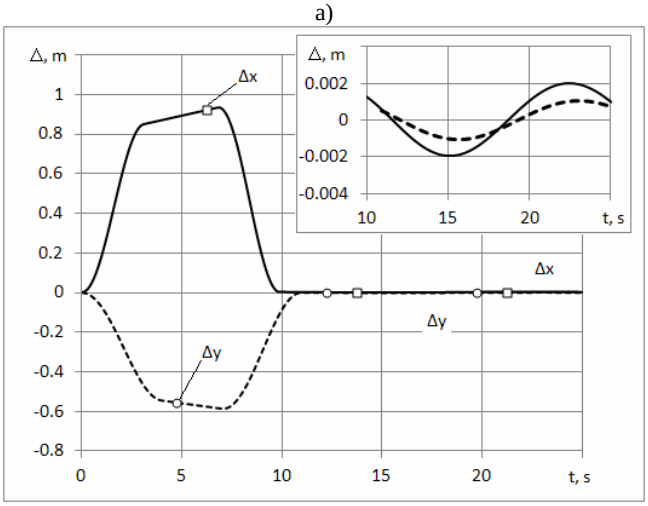

b)

Fig. 2. Illustration of the proposed method of damping the load oscillations when the operations of the load horizontal motion and lowering are combined: a) waveforms of the speed of the crane and the load, b) waveforms of the load deviation from the equilibrium (vertical) position

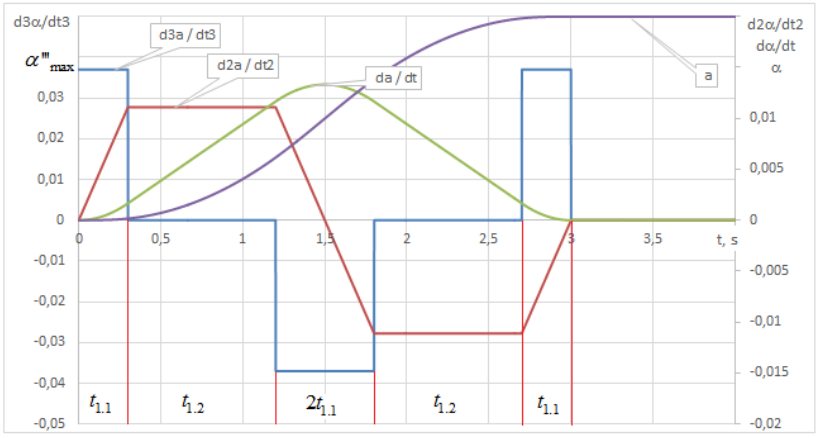

Fig. 3. Diagrams of the load sway angle α and its derivatives at the beginning of the acceleration of the traveling process

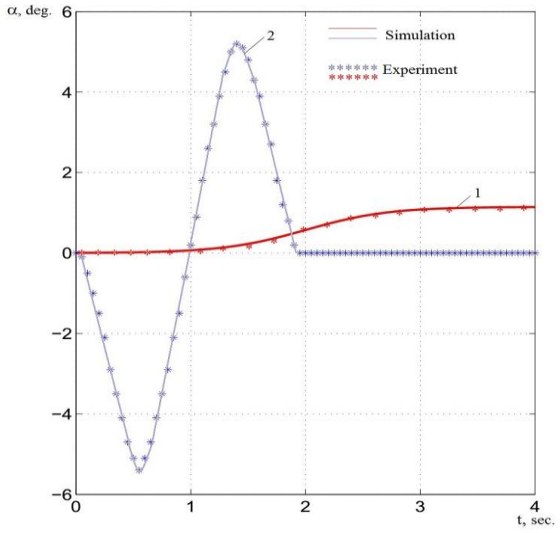

Fig. 4. Comparison between the proposed anti-sway system (curve 1) and neural anti-sway method (curve 2) given in [29]

It is important that the control system must set the duration of intervals $t_{1.1}, t_{1.2}$ and the amplitude of the third derivative $\alpha'''_{\max}$ based on the permissible rate of change and the maximum torque on the motor shaft. The other coordinates should be calculated by the controller using any method of numerical integration:

$$\begin{aligned} \alpha'' &= \frac{d^2\alpha}{dt^2} = \int_0^t \frac{d^3\alpha}{dt^3}\,dt, \\ \alpha' &= \frac{d\alpha}{dt} = \int_0^t \frac{d^2\alpha}{dt^2}\,dt, \\ \alpha(t) &= \int_0^t \frac{d\alpha}{dt}\,dt. \end{aligned} \tag{14}$$

To calculate the necessary parameters, the time intervals $t_{1.1} - t_{1.2} - t_{1.1}$ should be analyzed. For this interval, the following conditions should be satisfied:

$$0 \le \left|F(t)\right| \le F_{\max},$$
$$\alpha\big|_{t=2t_{1.1}+t_{1.2}} = \frac{\alpha_{\max}}{2}. \tag{15}$$

Based on the relationship $\alpha'''(t)$:

$$\alpha'''(t) = \begin{cases} \alpha'''_{\max} \ \forall\ 0 \le t \le t_{1.1}, \\ 0 \ \forall\ t_{1.1} \le t \le t_{1.1}+t_{1.2}, \\ -\alpha'''_{\max} \forall\ t_{1.1}+t_{1.2} \le t \le 2t_{1.1}+t_{1.2}, \end{cases} \tag{16}$$

We get:

$$\alpha''(t) = \alpha'''_{\max} \times \begin{cases} t \ \forall\ 0 \le t \le t_{1.1}, \\ t_{1.1} \ \forall\ t_{1.1} \le t \le t_{1.1}+t_{1.2}, \\ t_{1.1} - \left(t - \left(t_{1.1}+t_{1.2}\right)\right) \forall\ t_{1.1}+t_{1.2} \le t \le 2t_{1.1}+t_{1.2}, \end{cases}$$

$$\alpha'(t) = \alpha'''_{\max} \times \begin{cases} \frac{t^2}{2} \ \forall\ 0 \le t \le t_{1.1}, \\ \frac{{t_{1.1}}^2}{2} + t_{1.1}\left(t - t_{1.1}\right) \forall\ t_{1.1} \le t \le t_{1.1}+t_{1.2}, \\ \frac{{t_{1.1}}^2}{2} + t_{1.1}t_{1.2} + t_{1.1}\left(t - \left(t_{1.1}+t_{1.2}\right)\right) - \frac{\left(t-\left(t_{1.1}+t_{1.2}\right)\right)^2}{2} \forall\ t_{1.1}+t_{1.2} \le t \le 2t_{1.1}+t_{1.2}, \end{cases} \tag{17}$$

$$\alpha(t) = \alpha'''_{\max} \times \begin{cases} \frac{t^3}{6} \ \forall\ 0 \le t \le t_{1.1}, \\ \frac{{t_{1.1}}^3}{6} + \frac{{t_{1.1}}^2\left(t-t_{1.1}\right)}{2} + \frac{t_{1.1}\left(t-t_{1.1}\right)^2}{2} \ \forall\ t_{1.1} \le t \le t_{1.1}+t_{1.2}, \\ \frac{{t_{1.1}}^3}{6} + \frac{{t_{1.1}}^2 t_{1.2}}{2} + \frac{t_{1.1}{t_{1.2}}^2}{2} + \left(\frac{{t_{1.1}}^2}{2} + t_{1.1}t_{1.2}\right)\left(t-\left(t_{1.1}+t_{1.2}\right)\right) + \frac{t_{1.1}\left(t-\left(t_{1.1}+t_{1.2}\right)\right)^2}{2} - \\ -\frac{\left(t-\left(t_{1.1}+t_{1.2}\right)\right)^3}{6} \forall\ t_{1.1}+t_{1.2} \le t \le 2t_{1.1}+t_{1.2}, \end{cases}$$

In the boundary points, we get:

$$\alpha''(t) = \alpha'''_{\max} \times \begin{cases} t_{1.1} \ \forall\ t = t_{1.1}, \\ t_{1.1} \ \forall\ t = t_{1.1}+t_{1.2}, \\ 0 \ \forall\ t = 2t_{1.1}+t_{1.2}, \end{cases}$$

$$\alpha'(t) = \alpha'''_{\max} \times \begin{cases} \frac{{t_{1.1}}^2}{2} \ \forall\ t = t_{1.1}, \\ \frac{{t_{1.1}}^2}{2} + t_{1.1}t_{1.2} \ \forall\ t = t_{1.1}+t_{1.2}, \\ t_{1.1}t_{1.2} + {t_{1.1}}^2 \ \forall\ t = 2t_{1.1}+t_{1.2}, \end{cases} \tag{18}$$

$$\alpha(t) = \alpha'''_{\max} \times \begin{cases} \frac{{t_{1.1}}^3}{6} \ \forall\ t = t_{1.1}, \\ \frac{{t_{1.1}}^3}{6} + \frac{t_{1.1}{t_{1.2}}^2}{2} \ \forall\ t = t_{1.1}+t_{1.2}, \\ {t_{1.1}}^3 + \frac{3{t_{1.1}}^2 t_{1.2}}{2} + \frac{t_{1.1}{t_{1.2}}^2}{2} \ \forall\ t = 2t_{1.1}+t_{1.2}. \end{cases}$$

When $t = t_{1.1} + t_{1.2}$, the force reaches a maximum value; and when $t = 2t_{1.1} + t_{1.2}$, the deviation angle is equal to half of the maximum value. Given that $F_{\max} = (m_1 + m_2)\alpha_{\max} g$, at a constant length of the rope $(v_L = 0)$, equation (11) helps us get:

$$F(t) = (m_1 + m_2) g\alpha + m_1 \frac{d^2\alpha}{dt^2} L, \tag{19}$$

Then we get a system of equations:

$$\begin{cases} F_{\max} = (m_1 + m_2)\alpha_{\max} g = \alpha'''_{\max} (m_1 + m_2) g \left(\frac{t_{1.1}{}^3}{6} + \frac{t_{1.1} t_{1.2}{}^2}{2} \right) + \alpha'''_{\max} m_1 L t_{1.1} \ \forall\, t = t_{1.1} + t_{1.2}, \\ \frac{\alpha_{\max}}{2} = \frac{F_{\max}}{2(m_1 + m_2) g} = \alpha'''_{\max} \left(t_{1.1}{}^3 + \frac{3 t_{1.1}{}^2 t_{1.2}}{2} + \frac{t_{1.1} t_{1.2}{}^2}{2} \right) \forall\, t = 2t_{1.1} + t_{1.2}, \\ F' \big|_{t = t_{1.1}} = m_1 \alpha'''_{\max} L + (m_1 + m_2) g \alpha'''_{\max} \frac{t_{1.1}{}^2}{2}. \end{cases} \tag{20}$$

The first two equations can be rewritten as follows:

$$\begin{cases} \frac{F_{\max}}{\alpha'''_{\max} t_{1.1}} = (m_1 + m_2) g \frac{t_{1.1}{}^2}{6} + (m_1 + m_2) g \frac{t_{1.2}{}^2}{2} + m_1 L, \\ \frac{F_{\max}}{\alpha'''_{\max} t_{1.1}} = 2(m_1 + m_2) g t_{1.1}{}^2 + 3(m_1 + m_2) g t_{1.1} t_{1.2} + (m_1 + m_2) g t_{1.2}{}^2. \end{cases} \tag{21}$$

Equating the right-hand sides, we get:

$$11 t_{1.1}{}^2 + 18 t_{1.1} t_{1.2} + 3 t_{1.2}{}^2 - 6 \frac{m_1}{(m_1 + m_2) g} L = 0. \tag{22}$$

$$t_{1.1} = \frac{-18 t_{1.2} + \sqrt{192 t_{1.2}{}^2 + 264 \frac{m_1}{(m_1 + m_2) g} L}}{22}. \tag{23}$$

Substituting (23) in the first equation of (20), taking into account the third equation, the solution for $t_{1.1}$ can be found in an iterative manner as follows:

$$\frac{F_{\max} \left(m_1 L + (m_1 + m_2) g \frac{t_{1.1}{}^2}{2} \right)}{F'_{\max} t_{1.1}} = \\ = \frac{22}{3} (m_1 + m_2) g t_{1.1}{}^2 - 3(m_1 + m_2) g t_{1.1} \sqrt{\frac{32}{6} t_{1.1}{}^2 + 2 \frac{m_1}{(m_1 + m_2) g} L} + 2 m_1 L. \tag{24}$$

Based on the third equation of (20), $\alpha'''_{\max}$ equals:

$$\alpha'''_{\max} = \frac{F'_{\max}}{m_1 L + (m_1 + m_2) g \frac{t_{1.1}{}^2}{2}}. \tag{25}$$

Finally, from equation (22) $t_{1.2}$ is set to:

$$t_{1.2} = -3t_{1.1} + \sqrt{\frac{32}{6}{t_{1.1}}^2 + 2\frac{m_1}{(m_1+m_2)g}L}. \tag{26}$$

Thus, the transient parameters $\alpha'''_{max}, t_{1.1}, t_{1.2}$ are determined.

Further, equation (2) is used to calculate the load speed; and (3) calculates the speed of the suspension point, which in turn will be used as a speed setpoint signal in the control system of the traveling mechanism.

Fig. 5 shows diagrams corresponding to the acceleration of the traveling mechanism at a constant length of the rope; and Fig. 6- combines the operations of the horizontal motion and lifting, respectively.

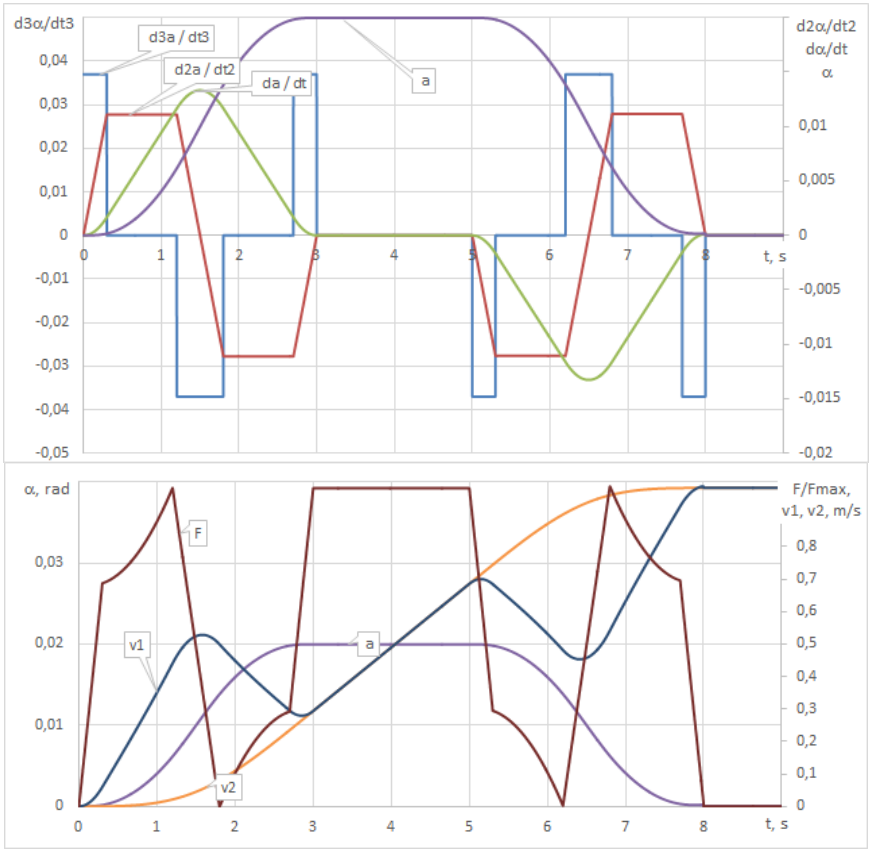

Fig. 5. Waveforms of the load and suspension point speed, force and the load angle of deviation and its derivatives in accordance with Fig. 3

Based on Fig. 5 and 6, no step-changes in the force are required for anti-sway control. This helps reduce shock loads in the drive of the crane, increase the accuracy of control, and coordinate the rate of change of force (motor torque) with the capabilities of the drive system.

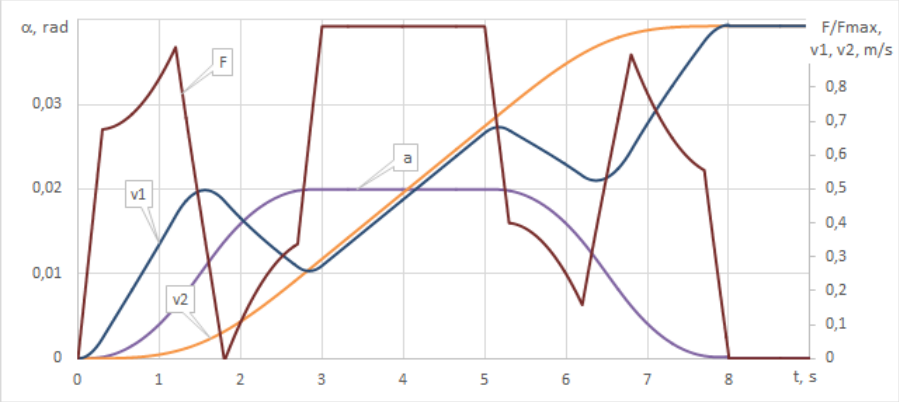

Fig. 6. Waveforms of the speed of the load, suspension point and motor torque/force for a lowering process at 1m/s

Fig. 7 illustrates the load speed, suspension point speed, force and the load deviation angle waveforms for a load traveling process.

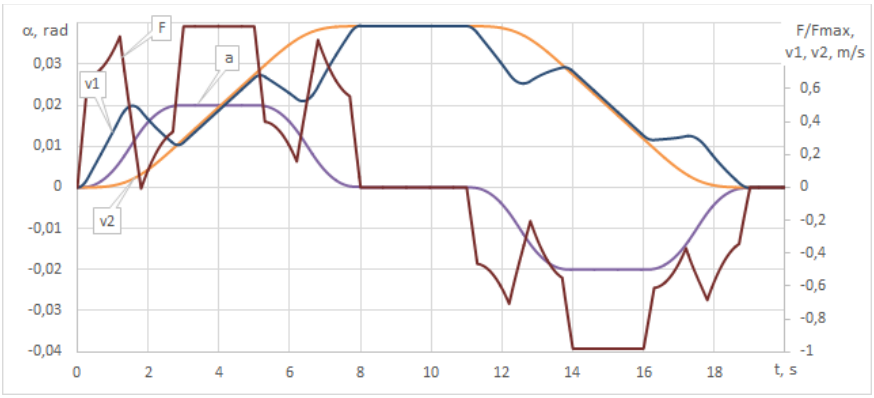

Fig. 7. Waveforms of the load speed, suspension point speed, force and the load deviation angle for a load traveling process

A distinctive feature of the proposed anti-sway control methodology is the constancy of the sign of the force (motor torque) during the transient. This makes this method physically realizable in modern VFD or DTC systems.

V. EXPERIMENTAL SETUP AND RESULTS

In order to validate the simulation results, a container crane prototype with a lifting height of 1m and a jib length of 1.5m is designed. A photograph of the experimental setup of the container crane is shown in Fig. 8. Stepper motors are used in the trolley and hoist drives. The motors are connected through a 4-q and 2-phase drivers to the controller using the protocol Modbus, which is connected to SCADA Mitsubishi Electric Citect 7.x. The measurement and control of the experimental setup are implemented on a DSP board with a sampling time of 2ms.

The motion algorithm is generated in the SCADA system; and the motion coordinates are demonstrated online on the screen. In addition, the visual observation of the load sway is a major factor in estimating the control system performance.

Two case studies are experimentally demonstrated below. In Fig. 9, a stopping process of two simultaneous operations (trolley horizontal motion and load hoist) is manually performed; the load sway is clear on the corresponding waveforms. A complete motion cycle including starting of the hoist/trolley drives, load translation and stopping is performed using the proposed anti-sway control method. The experimental results of this case study are depicted

in Fig. 10. The corresponding waveforms show that the load sway is significantly damped by the end of the starting and stopping. The visual observation of the load behavior confirms the absence of the load sway as well.

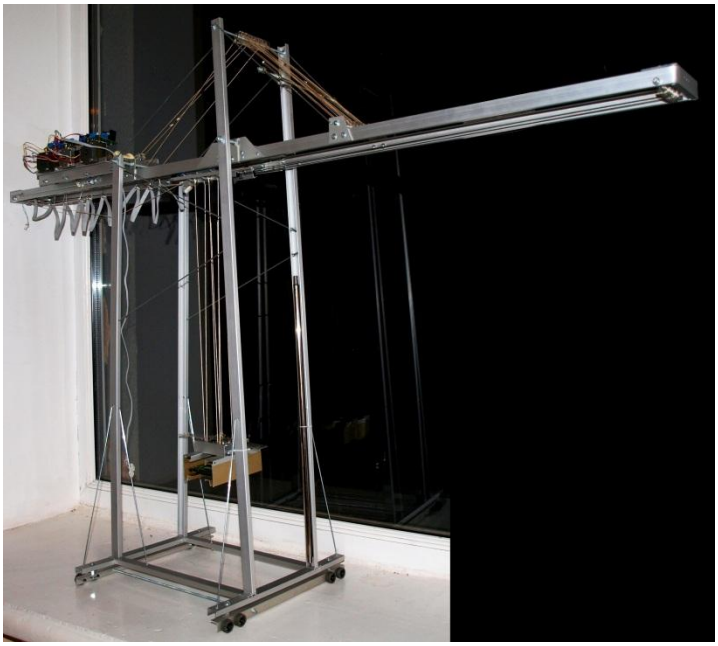

Fig. 8. Photograph of the experimental setup of the container crane

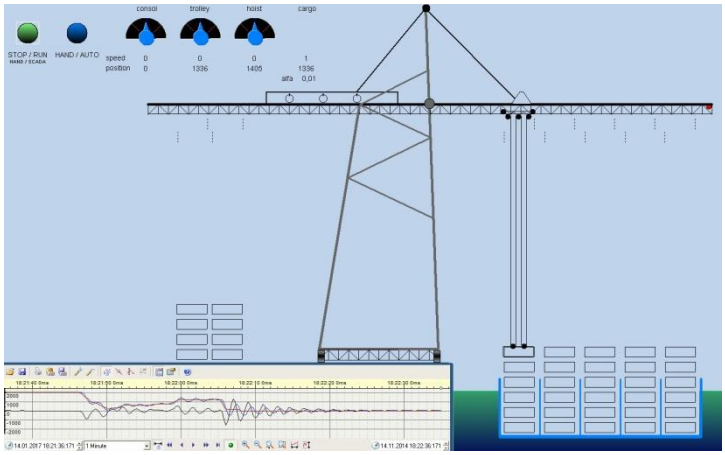

Fig. 9. Experimental results for a stopping transient without anti-sway control

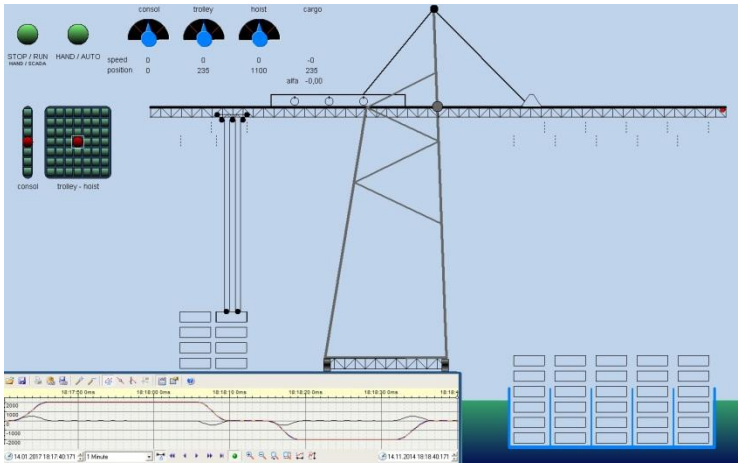

Fig. 10. Experimental results for the crane complete stroke: starting, load translation and stopping with anti-sway control

VI. CONCLUSIONS

1. Experimental and simulation results show that the load sway disappears by the end of any transient process with simultaneous horizontal load motion (in two orthogonal coordinates) and vertical load motion (lifting/lowering).
2. The coincidence of the theoretical and experimental results proves the validity of the mathematical model on which the simulation is based. It also proves the effectiveness of the proposed anti-sway control methodology.
3. A novel speed control method for the suspension point of the cargo in container cranes is proposed. The proposed method provides damping of the oscillations of the suspended load during its horizontal motion (in two orthogonal coordinates) and lifting/lowering. The control method is invariant to the mechanism/cargo mass ratio and to the hoisting speed.
4. Controlling the speed of the load suspension point permits selecting the parameters of the transient processes in a wide range based on the requirements and limitations of dynamic loads and response.
5. The proposed control method is based on the formation of a predetermined angle of deviation as a piecewise-continuous function, the second derivative of which does not experience discontinuity. Its third derivative is a rectangular pulse of a certain variable-sign amplitude, which eliminates the mechanical stress in the crane construction and kinematic gears.
6. A distinctive feature of the proposed anti-sway control methodology is the constancy of the sign of the force (motor torque) during the transient. This makes this method physically realizable in modern VFD or DTC systems.
7. Based on the formulated speed diagrams of the mechanism and load during starting and braking, the system's safety increases; and the smoothness of motion permits the crane automated operation, including precised positioning of the load in predetermined points. Such automated operation can be implemented in the design of container cranes working in automated terminals.

REFERENCES

[1] E. Abdel-Rahman, A. Nayfeh, and Z. Masoud, "Dynamics and control of cranes: a review," *Vibration and Control*, vol. 9, pp. 863-908, 2003.

[2] Y. Fang, W. Dixon, D. Dawson, and E. Zergeroglu, "Nonlinear coupling control laws for an underactuated overhead crane system," *IEEE/ASME Transactions on Mechatronics*, vol. 8, no. 3, pp. 418-423, 2003.

[3] B. Ma, Y. Fang, and Y. Zhang, "Switching-based emergency braking control for an overhead crane system," *IET Control Theory and Applications*, vol. 4, no.9, pp. 1739-1747, 2010.

[4] N. Sun, Y. Fang, X. Zhang, and Y. Yuan, "Phase plane analysis based motion planning for underactuated overhead cranes," *Proceedings of 2011 IEEE Conference on Robotics and Automation*, pp. 3483-3488, 2011.

[5] W. Yu, M. Moreno-Armendariz, and F. Rodriguez, "Stable adaptive compensation with fuzzy CMAC for an overhead crane," *Information Sciences*, vol. 181, no. 21, pp. 4895-4907, 2011.

[6] N. Sun and Y. Fang, "New energy analytical results for the regulation of underactuated overhead cranes: an end-effector motion-based approach," *IEEE Transactions on Industrial Electronics*, vol. 59, no. 12, pp. 4723-4734, 2012.

[7] D. Kim, Y. Park, and Y.-S. Park, "Feasibility test of tracking control to moving target in dual-stage trolley control system," *Proceedings of the Control, Automation and Systems Conference*, pp. 235-239, 2012.

[8] Y. Zhao and H. Gao, "Fuzzy-model-based control of an overhead crane with input delay and actuator saturation," *IEEE Transactions on Fuzzy Systems*, vol. 20, no.1, pp. 181-186, 2012.

[9] N. Sun and Y. Fang, "Nonlinear tracking control of underactuated cranes with load transferring and lowering: theory and experimentation," *Automatica*, vol. 50, no. 9, pp. 2350-2357, 2014.

[10] Y. Fang, P. Wang, N. Sun, and Y. Zhang, "Dynamics analysis and nonlinear control of an offshore boom crane," *IEEE Transactions on Industrial Electronics*, vol. 61, no. 1, pp. 414-427, 2014.

[11] Z. Wu and X. Xia, "Model predictive control for improving operational efficiency of overhead cranes," *Nonlinear Dynamics*, vol. 19, no. 4, pp. 2639-2657, 2015.

[12] Z. Masoud, A. Nayfeh, and D. Mook, "Cargo pendulation reduction of ship-mounted cranes," *Nonlinear Dynamics*, vol. 35, no. 3, pp. 299-311, 2004.

[13] Z. Masoud, M. Daqaq, and N. Nayfeh, "Pendulation reduction on small ship-mounted telescopic cranes," *Vibration and Control*, vol. 10, pp. 1167-1179, 2004.

[14] H. Schaub, "Rate-based ship-mounted crane payload pendulation control system," *Control Engineering Practice*, vol. 16, no. 1, pp. 132-145, 2008.

[15] K. Khandakji and K. Zdrozis, "Optimum sway control for overhead traveling cranes," *WSEAS Transactions on Circuits and Systems*, vol. 7, no.6, pp. 521-527, 2008.

[16] S. Garrido, M. Abderrahim, A. Giménez, R. Diez, and C. Balaguer, "Anti-swinging input shaping control of an automatic construction crane," *IEEE Transactions on Automation Science and Engineering*, vol. 5, no. 3, pp. 549-557, 2008.

[17] M. Park, D. Chwa, and S. Hong, "Antisway tracking control of overhead cranes with system uncertainty and actuator nonlinearity using an adaptive fuzzy sliding-mode control," *IEEE Transactions on Industrial Electronics*, vol. 55, no. 11, pp. 3972-3984, 2008.

[18] D. Chwa, "Nonlinear tracking control of 3-D overhead cranes against the initial swing angle and the variation of payload weight," *IEEE Transactions on Control Systems Technology*, vol. 17, no. 4, pp. 876-883, 2009.

[19] K. Terashima, R. Ito, Y. Noda, Y. Masui, and T. Iwasa, "Innovative integrated simulator for agile control design on shipboard crane considering ship and load sway," *Proceedings of IEEE Control Applications Conference*, pp. 1293-1300, 2010.

[20] D. Kim, Y. Park, Y.-S. Park, S. Kwon, and E. Kim, "Dual stage trolley control system for anti-swing control of mobile harbour crane," *Proceedings of the Control, Automation and Systems Conference*, pp. 420-423, 2011.

[21] Q. Ngo and K. Hong, "Sliding-mode antisway control of an offshore container crane," *IEEE/ASME Transactions on Mechatronics*, vol. 17, no. 2, pp. 201-209, 2012.

[22] Q. Ngo and K. Hong, "Adaptive sliding mode control of container cranes," *IET Control Theory and Applications*, vol. 6, no. 5, pp. 662-668, 2012.

[23] L. Tuan, S. Moon, W. Lee, and S. Lee, "Adaptive sliding mode control of overhead cranes with varying cable length," *Mechanical Science and Technology*, vol. 27, no. 3, pp. 885-893, 2013.

[24] M. Park, D. Chwa, and M. Eom, "Adaptive sliding-mode antisway control of uncertain overhead cranes with high-speed hoisting motion," *IEEE Transactions on Fuzzy Systems*, vol. 22, no. 5, pp. 1262-1271, 2014.

[25] D. Jolevski and O. Bego, "Model predictive control of gantry/bridge crane with anti-sway algorithm," *Mechanical Science and Technology*, vol. 29, no. 2, pp.827-834, 2015.

[26] Z. Zhang, Y. Wu, and J. Huang, "Differential-flatness-based finite-time anti-swing control of underactuated crane systems," *Nonlinear Dynamics*, vol. 87, no. 3, pp. 1749-1761, 2017.

[27] M. Ermidoro, A. Cologni, S. Formentin, and F. Previdi, "Fixed-order gain-scheduling anti-sway control of overhead bridge cranes," *Mechatronics*, vol. 39, pp.237-247, 2016.

[28] V. Busher, L. Melnikova, and A. Shestaka, "Coordinated control of simultaneous operation of container crane mechanisms," *Electrotechnic and Computer Systems*, vol. 19, pp. 58-61, 2015.

[29] A. Abe, "Anti-sway control for overhead cranes using neural networks," *Innovative Computing, Information and Control*, vol. 7, no. 7, pp. 4251-4262, 2011.